Atmos. Meas. Tech. Discuss., 5, 385–409, 2012
www.atmos-meas-tech-discuss.net/5/385/2012/
doi:10.5194/amtd-5-385-2012
© Author(s) 2012. CC Attribution 3.0 License.

Atmospheric Measurement Techniques Discussions

This discussion paper is/has been under review for the journal Atmospheric Measurement Techniques (AMT). Please refer to the corresponding final paper in AMT if available.

Atmospheric effect on the ground-based measurements of broadband surface albedo

T. Manninen[1], **A. Riihelä**[1], **and G. de Leeuw**[1,2]

[1]Finnish Meteorological Institute, P.O. Box 503, 00101 Helsinki, Finland
[2]Department of Physics, P.O. Box 64, University of Helsinki, 00014 Helsinki, Finland

Received: 20 December 2011 – Accepted: 2 January 2012 – Published: 11 January 2012

Correspondence to: T. Manninen (terhikki.manninen@fmi.fi)

Published by Copernicus Publications on behalf of the European Geosciences Union.

Abstract

Ground-based pyranometer measurements of broadband surface albedo values are affected by the atmospheric conditions. A new method for estimating the magnitude of this effect in clear sky conditions is presented. Global and reflected radiation values and AOD values at two wavelengths are needed to apply the method. Depending on the atmospheric optical depth and the sun zenith angle values the effect can be as large as 20 %. For the test case of Cabauw the atmosphere caused typically 5 % higher surface albedo values than the corresponding black-sky surface albedo values.

1 Introduction

Satellite Application Facilities (SAFs) are specialized development and processing centres within the EUMETSAT Applications Ground Segment. The Satellite Application Facility on Climate Monitoring (CM SAF) was initiated in order to generate and archive high quality data sets for climate monitoring and modelling (Schulz et al., 2009). One of the CM SAF products is the surface albedo product (SAL), which is defined to be the black-sky broadband albedo normalized to sun zenith angle of 60°. Satellite based surface albedo products require long term validation based on continuous surface albedo measurements, which need to be made with the highest possible accuracy and free of atmospheric influence. The validation of the SAL product has two main strategies: large areas are validated with airborne measurements instantaneously or individual pixels are validated with continuous ground-based measurement results during long periods, preferably covering seasonal variation (Riihelä et al., 2010).

The black-sky and white-sky albedo quantities represent the extreme cases under completely direct and completely diffuse illumination (Pinty et al., 2005; Román et al., 2010). In addition, the black-sky albedo is understood to match the case, when no atmosphere exists. I.e. it is a property of only the surface (and the illumination spectrum of the sun). The atmospheric correction of satellite images has been studied since

AMTD
5, 385–409, 2012

several decades and various solutions for taking into account the atmospheric effects on the albedo have been proposed (Martonchik et al., 1998; Strahler et al., 1999; Govaerts et al., 2006; Pinty et al., 2007; Carrer et al., 2009; Rahman and Dedieu, 1994; Lyapustin et al., 2011a,b). In addition, the influence of the sky radiance distribution, including the effect of aerosols, on the spectral albedo has been studied in detail (Lewis and Barnsley, 1994). The emphasis has been on the difference between the albedo values obtained in clear sky (blue-sky), diffuse sky (white-sky) and without atmosphere (black-sky) conditions.

Validation of the black-sky and white-sky albedo values is complicated by the fact that neither the satellite nor the ground based instrument can measure the surface black-sky albedo because of the atmosphere and the satellite instrument cannot measure the surface white-sky albedo because of the cloud cover. Only the blue-sky albedo can be observed both by the satellite and the ground based instruments. The quality assessment of satellite based black-sky and white-sky albedo values is often based on estimating the accuracy of the blue-sky value and then relating this accuracy theoretically to the black-sky and white-sky albedo accuracy (Román et al., 2010).

Another perspective is to study the effect of the atmosphere on the ground measurements separately and derive estimates for the difference between the black-sky and blue-sky albedo values for them. This analysis is completely independent of the chosen satellite instrument. The advantage of this approach is that one does not have to tackle the effect of the atmosphere and the spatial land cover heterogeneity simultaneously, when comparing satellite and ground based albedo estimates. Especially when using a relatively coarse resolution satellite instruments, such as AVHRR, this is important.

The broadband surface albedo is measured continuously at several permanent locations using pyranometers, for example by the BSRN network (Ohmura et al., 1998; WRCP, 2007). A pyranometer senses the heating power of broadband solar irradiance on a planar surface. It is designed to measure the solar radiation flux density (in watts per square metre) from a field of view of 180°. Instrumental error sources

AMTD
5, 385–409, 2012

of pyranometers have been studied for decades and are well known (Michalsky et al., 1995; Raïch et al., 2007). Typically the spectral response is good and the cosine correction, which takes into account the difference between the angular response of a pyranometer in ideal conditions (i.e. vacuum) and in the atmosphere, is essential only when the sun zenith angle is larger than 60°. Pyranometer measurements used for the validation of satellite-retrieved surface albedo estimates require attention to leveling accuracy, nonperfect cosine response, solar zenith angle and soil moisture effects (Lucht et al., 2000). The effect of the atmospheric optical depth on the pyranometer-measured irradiance has so far not been studied, because it is important only when pyranometers are used for surface characterisation such as albedo measurements. The albedo values obtained using pyranometers contain contributions from the atmosphere, because the surface irradiance spectra are modified by atmospheric absorption and scattering. The main problem is varying cloud cover, but even in completely clear sky conditions the surface irradiance spectra have a different shape than those at the top of atmosphere (TOA). Since the surface albedo is generally wavelength dependent the broadband albedo value obtained is different from the value that one would obtain without the atmosphere (Manninen and Riihelä, 2008). In this paper we show that variations of up to 20 % may occur. This is undesirable because ground-based albedo measurements are used as ground truth for satellite validations in addition to dedicated field campaigns (Liang et al., 2002).

This conclusion is based on simulations of the atmospheric contribution to the surface albedo that would be obtained by ground-based pyranometer reflectance spectra measurements for a range of land cover types, various sun zenith angles and typical aerosol optical depth (AOD) values. The direct and diffuse irradiance values are obtained from the SPCTRAL2 model (Bird and Riordan, 1986; Gueymard, 1995, 2001) with the ASTM Standard G173-03 as input for the TOA solar spectral irradiance. In addition, a robust regression formula is derived for the relationship of the simulated pyranometer-measured surface albedo and the corresponding black-sky albedo. This formula is then applied to albedo and AOD measured at the BSRN Cabauw site in

AMTD
5, 385–409, 2012

order to estimate the magnitude of the atmospheric correction related to real albedo data.

2 Materials

The atmospheric effect on measured surface albedo is simulated for 87 individual reflectance spectra of diverse land cover types which were selected from the USGS Spectral lab data base: 10 for grass, 19 for forest, 5 for crop, 6 for lichen, 4 for minerals, 18 for man-made materials, 4 for water, 8 for snow/ice and 13 for mixtures of rock etc. (Clark et al., 2007). The spectra are shown in Fig. 1.

AOD measured at Cabauw on clear days during January–July 2007 is available at four wavelengths (440 nm, 675 nm, 870 nm and 1020 nm) via AERONET (Holben et al., 1998). Values for two wavelengths are shown as a function of the sun zenith angle in Fig. 2. A wide variation of the AOD is observed at all angles, which allows studying the effect of the AOD and the sun zenith angle separately. Also the largest AOD values are very high, so that the data set is able to demonstrate the effect of aerosols very well. Therefore the AOD values measured in Cabauw were used in the simulation of the atmospheric effect.

Simultaneously measured broadband albedo (Knap, http://www.knmi.nl/bsrn/) and AOD are available for Cabauw thus allowing for estimation of the magnitude of the atmospheric effect on real data. The albedo measurements are carried out using pyranometers of the highest available accuracy and with high time resolution (1 to 3 min). The measurement site is completely flat grassland. The albedo values were normalized to a sun zenith angle of 60° using (Briegleb et al., 1986):

$$\alpha_n = \alpha \frac{1 + 2 \times f \cos \theta_z}{1 + f}. \quad (1)$$

Here α is the measured broadband albedo, α_n the normalized albedo, θ_z the sun zenith angle and f a coefficient related to the land cover class. For Cabauw the value $f = 0.22$, corresponding to grass, was used.

AMTD
5, 385–409, 2012

The normalized albedo values are shown in Fig. 3 as a function of the AOD for wavelengths 440 nm and 870 nm. As expected the AOD value range starts from smaller values for the larger wavelength. Obviously the variation of the AOD value in Cabauw is large for both wavelengths. In addition, there is no marked correlation between the surface albedo and the AOD values so that the seasonal variation of the surface and the atmospheric aerosol load are relatively independent. Thus the data set of Cabauw is well suited for the testing the atmospheric effect estimation to be developed on the measured broadband surface albedo.

3 Simulation of the atmospheric effect on the broadband surface albedo

The broadband surface albedo α_{bb} is the ratio of the total reflected radiation and the incoming radiation. In practice only the shortwave part of the spectrum (300 nm–2500 nm) is taken into account. Pyranometers usually measure the total radiation integrated over the bandwidth 305 nm–2800 nm. The reflected short wave radiation R_{sw} is related to the short wave irradiance I_{sw} the spectral albedo $\alpha(\lambda)$ and reflectance $r(\lambda)$ via

$$\alpha_{bb} = \frac{R_{sw}}{I_{sw}} = \frac{\int \alpha(\lambda)\, I(\lambda)\, d\lambda}{\int I(\lambda)\, d\lambda} = \frac{\int r(\lambda)\ \mathrm{BRDF}\ (\theta_z, \theta, \varphi_z, \varphi, \lambda)\, I(\lambda)\, d\lambda}{\int I(\lambda)\, d\lambda} \quad (2)$$

where the bidirectional reflectance distribution function BRDF $(\theta_z, \theta, \varphi_z, \varphi, \lambda)$ describes which fraction of the reflected radiation coming from direction (θ_z, φ_z) is reflected to the direction (θ, φ), where θ_z and φ_z are the sun zenith and azimuth angles and θ and φ are the zenith and azimuth angles of the viewing direction. The BRDF is not typically a strong function of the wavelength, but slightly different values are often obtained for the visible and near infrared wavelengths.

If there were no atmosphere the irradiance used in Eq. (2) would be the top of atmosphere solar spectral irradiance $I_0(\lambda)$ (ASTM Standard G-173-03) and the broad band albedo would be the black-sky albedo α_{0bb}. However, the presence of aerosol particles

AMTD
5, 385–409, 2012

and gases in the atmosphere requires that both the direct and diffuse contributions to the irradiance at the surface are taken into account.

Surface albedo values measured at grazing incidence angles are typically very noisy and values measured at sun zenith angles larger than 70° are usually discarded from analysis. In that case the attenuation by the atmosphere can quite accurately be taken into account by assuming that the light propagates in the atmosphere along a straight path. Then the direct solar irradiation at the surface per unit area $I_{\mathrm{dir}}(\lambda)$ is related to the irradiation at the top of the atmosphere $I_0(\lambda)$ by (Bird and Riordan, 1986)

$$I_{\mathrm{dir}}(\lambda) = I_0(\lambda) \exp\left(-\tau_{\mathrm{a}}(\lambda)/\cos\theta_{\mathrm{z}}\right) \cos\theta_{\mathrm{z}} \tag{3}$$

where θ_{z} is the sun zenith angle and $\tau_{\mathrm{a}}(\lambda)$ is the aerosol optical depth (AOD), which depends on the wavelength according to (Ångström, 1929)

$$\tau_{\mathrm{Aer}}(\lambda) = \beta \cdot \lambda^{-\alpha_{\mathrm{A}}} = \tau_{\mathrm{Aer}}(\lambda_{\mathrm{ref}}) \cdot \left(\frac{\lambda}{\lambda_{\mathrm{ref}}}\right)^{-\alpha_{\mathrm{A}}}, \tag{4}$$

where $\tau_{\mathrm{Aer}}(\lambda)$ is the AOD at wavelength λ, β is the AOD at the reference wavelength λ_{ref} (usually taken at 1 µm) and α_{A} is the Ångström exponent evaluated for the wavelength pair λ_1 and λ_2. An example set of AOD values was derived for the simulations by regression of Eq. (4) to the measured AOD values at wavelengths of 440 nm, 675 nm, 870 nm and 1020 nm. The regression was carried out separately for each quartet of recorded AOD values. Altogether there were 2226 quartets resulting in 2226 regression functions $\tau_{\mathrm{Aer}}(\lambda)$.

The estimation of the diffuse solar irradiation at the surface per unit area $I_{\mathrm{diff}}(\lambda)$ is much more complex. Because the motivation for this work is to derive the atmospheric correction for ground-based measurements, which in turn are used for validation of satellite-based albedo estimates, only clear sky cases are of interest. In addition, ground-based surface albedo measurements are usually not accompanied by simultaneous aerosol measurements which allow for an accurate atmospheric correction. Therefore a relatively simple but informative model, using only a limited and readily

AMTD
5, 385–409, 2012

available number of atmospheric parameters, would be desirable to estimate the diffuse irradiation. The model SPCTRAL2 (Bird and Riordan, 1986; Gueymard, 1995, 2001) was chosen for that reason.

The diffuse irradiance computed in SPCTRAL2 consists of three components: (1) Rayleigh scattering, (2) aerosol scattering and (3) a component that accounts for multiple scattering of light between the ground and the atmosphere. The diffuse irradiance component contains separate transmittance terms for ozone, water vapour, mixed gas and aerosol absorption and for aerosol scattering.

The absorption bands of ozone and water vapour are mainly situated at longer wavelengths, so that the exact amount of ozone and water vapour are not crucial for the total broad band irradiance in clear sky cases. Therefore in the simulations the ozone and water vapour contributions are taken to be equal to those of the standard atmosphere (ASTM Standard G173-03).

The simulated broadband albedo that would be measured by a pyranometer is then obtained using the sum of the modelled direct I_{dir} and diffuse I_{diff} radiation for the irradiance I_{sw} in Eq. (2). The required reflectance spectra are directly derived from the USGS Spectroscopy Lab database (Clark et al., 2007). Then only the BRDF is needed to obtain the surface albedo estimate.

At this stage the idea is to simulate the variation range of the atmospheric effect for a chosen example set of land cover spectra, which covers the wide variation of typical land cover types. Therefore, it is not critical to have the BRDF description for the chosen individual model targets, which are just random representatives of similar targets, but the BRDF descriptions have to be realistic both in size and in characteristics. The BRDF values were obtained using the methods developed for visible and near infrared bands of satellite instruments (Roujean et al., 1992; Wu et al., 1995). The spectra were split into a visible and an infrared part separated at 750 nm.

The total, visible and near-infrared irradiance values (I_{0sw}, I_{0vis} and I_{0nir}) at the top of the atmosphere are obtained by integrating the solar irradiance spectra (ASTM Standard G173-03) over 305 nm–750 nm for the visible band and over 750 nm–2500 nm

AMTD
5, 385–409, 2012

for the near infrared band. Pyranometers usually measure the irradiance integrated over the band 305 nm–2800 nm, but the irradiance in the band 2500 nm–2800 nm is negligible (<0.2 %) compared to the whole irradiance or that of the near infrared band.

The simulated broad band surface albedo values that a pyranometer would observe were then compared to the corresponding simulated black-sky surface albedo values in order to assess the effect of the atmosphere on the albedo observation. A typical cosine correction was also calculated to check its effect on the results (Michalsky et al., 1995). The uncorrected global irradiance is just the sum of the direct I_{dir} and diffuse I_{diff} irradiance values. The cosine corrected irradiance I_{c} was obtained from

$$I_{\mathrm{c}} = \left(1 + \frac{I_{\mathrm{diff}}}{1367 \cos\theta_{\mathrm{z}}}\right) I_{\mathrm{dir}}\, C_{\mathrm{bTP}} + \left(1 - \frac{I_{\mathrm{dir}}}{1367 \cos\theta_{\mathrm{z}}}\right) I_{\mathrm{diff}}\, C_{\mathrm{bTP}}. \quad (5)$$

The correction coefficient C_{bTP} values for all sun zenith angle were interpolated/extrapolated from the values given by Michalsky et al. (1995) for 0, 10, 20, 30, 40, 50, 60 and 70°.

4 Results

Aerosols affect the direct and diffuse components of the irradiance in opposite ways. The larger the AOD, the smaller is the amount of direct radiation reaching the surface, but the larger is the proportion of the diffuse radiation. The atmospheric effect is most evident at the shortest wavelengths because the AOD is usually largest at the shorter wavelengths. Also the increase of the sun zenith angle results in decrease of the direct irradiance and increase of the fraction of diffuse irradiance due to the longer atmospheric path.

The calculated broad band black-sky albedo is shown in Fig. 4a as a function of the simulated pyranometer measurement of the broad band surface albedo for all studied land cover types and AOD values. The effect of varying AOD (Fig. 2) manifests in the horizontal variation range of the simulated blue-sky albedo values corresponding to

AMTD
5, 385–409, 2012

each calculated black-sky albedo value. Although the effect of the atmosphere is not large in the standard atmosphere (ASTM Standard G173-03) the whole range of AOD values measured at Cabauw cause a drastic variation in the simulated values. Without quantifying the atmospheric effect this kind of data would be problematic for validation of satellite products. Fitting radiative transfer equations simultaneously to the surface and the atmosphere might not produce good results, when the AOD values are large.

Taking a subset of only grass spectra does not improve the situation much (Fig. 4b). The difference between the simulated pyranometer-measured surface albedo and the corresponding black-sky albedo depends on the sun zenith angle, overestimations being more common at small sun zenith angle values, but the variation range is about the same for all angles (Fig. 5). The effect of the atmosphere can be as large as 20 %. For small sun zenith angle values the atmosphere causes typically overestimation of the black-sky albedo, whereas for sun zenith angle of the order of 70° underestimation is more common. In the Cabauw data the atmospheric optical depth in most cases decreases with increasing wavelength. Therefore near-infrared irradiance is less attenuated than that at shorter wavelengths and thus the spectrum at the surface changes from that at the top of the atmosphere with a relatively lower intensity in the near-infrared part of the spectrum. On the other hand for most of the studied spectra the reflectance is higher in the near-infrared region than in the visible region. This resulted in a larger fraction of reflected radiation than would have been, if the irradiance spectrum had been equal to that of the TOA irradiance. The only target which has a clearly smaller reflectance in the near infrared band than in the visible band, was snow. Accordingly snow albedo was mostly underestimated also in low sun zenith angle cases. However, one has to take into account that the simulated result corresponds to an ideal pyranometer. The cosine correction is largest at large sun zenith angle values and typically such, that it would lead to overestimation of the albedo (Michalsky et al., 1995). A typical cosine correction would shift the error points of Fig. 5 corresponding to the sun zenith angle value 70° a few percent upwards.

AMTD
5, 385–409, 2012

Due to the complex nature of the diffuse radiation component and the varying shapes of the diverse land cover type spectra it is not possible to derive a simple analytic relationship between the black-sky surface albedo α_{0bb} and the simulated surface albedo α_{bb}. Therefore an empirical regression of the form $\alpha_{bb}\,(1+...)$ was sought. The parameters included were the AOD values at two wavelengths (τ_{440} and τ_{870}), the sun zenith angle (θ_z) and the direct (I_{dir}) and diffuse (I_{diff}) irradiance and the mathematical form of their appearance is sought to resemble expressions in the diffuse radiation components (Bird and Riordan, 1986). The obtained relationship is

$$\hat{\alpha}_{0bb} = \alpha_{bb}\left[1 + c_1\,\frac{\left(1-\exp\left(-\tau_{440}/\cos\theta_z\right)\right)}{1-\alpha_{bb}} + c_2\,\frac{\left(1-\exp\left(-\tau_{870}/\cos\theta_z\right)\right)}{\cos\theta_z}\right.$$
$$\left. + c_3\,\frac{I_{dir}\left(1-\exp\left(-\tau_{440}/\cos\theta_z\right)\right)}{\cos\theta_z^2} + c_4\,I_{diff}\right]. \quad (6)$$

The regression parameter values are given in Table 1 and the coefficient of determination for the regression was 0.999, when all AOD values and all spectra were included in the regression. The individual correction terms equal zero, when the AOD = 0, because then $\tau_{440}=0$, $\tau_{870}=0$ and $I_{diff}=0$, so that the estimate approaches the black-sky value properly.

The black-sky albedo estimation (Eq. 6) was applied to the studied land cover spectra, and it turned out that the absolute difference between the estimate and the true value was quite small (Fig. 6). The estimation accuracy decreases when the sun zenith angle exceeds 60°. The mean and the relative mean accuracy of the estimated black-sky albedo are shown in Fig. 7. Obviously the atmospherically corrected albedo estimate is on average within 0.005 of the black-sky value, whereas the uncorrected albedo deviates roughly 0.01 from it. However, more important is that the atmospheric correction removes large errors so that the deviation from the true value is in 90 % of the cases smaller than 0.015 and the relative error is smaller than 8 %. For the

AMTD
5, 385–409, 2012

uncorrected albedo the corresponding deviations are 0.03 and 11 %. The largest difference between the simulated pyranometer-measured albedo and the corresponding black-sky value was at nadir 0.09, which was reduced to 0.044 by the atmospheric correction. Although large sun zenith angle values (~70°) are problematic for measurements (for cosine response for example), the atmospheric effect is non-negligible also when the sun elevation is high.

The derived atmospheric correction method was then tested with real data using simultaneous albedo and AOD measurements at Cabauw. The atmospherically corrected albedo values were obtained by application of Eq. (6) to the measured incoming and reflected radiation, AOD and sun zenith angle values. It turned out that the atmosphere typically increased the albedo of the order of 5 % (relative) (Fig. 8). The atmospheric correction decreased the average albedo from 0.26 to 0.25, but the standard deviation increased at the same time from 3.5 % to 4.0 %. Evidently the normalization of the broadband albedo using the parameter value $f = 0.22$ in Eq. (1) is derived for a typical atmosphere. If the parameter f would be given a value of 0.3, the normalization would be suited to the atmospherically corrected albedo values at Cabauw. In that case the mean albedo value would still be 0.25, but the standard deviation would match the original value of 3.5 %.

The atmospheric correction presented requires besides the normal pyranometer measurements (global irradiance and reflected radiation) only AOD values for at least two wavelengths to determine the spectral behaviour (Eq. 6). No BRDF is needed when using the model. The direct solar irradiation can be calculated from the sun zenith angle and the solar constant, when the AOD is known (Eq. 3). Then the diffuse component is the difference of the measured global irradiance and the direct solar irradiance.

The regression parameters presented here were derived to be applicable to various kinds of land cover spectra. For permanent measurement sites one might improve the accuracy if the spectra used in the simulations were replaced with spectra specific for that site. Also the sun zenith angle effect could be better taken into account, if the

AMTD
5, 385–409, 2012

regression parameters were derived separately for all angles. Yet the current method with constant coefficient values can be applied to estimating the size of the effect of the atmosphere on the broadband surface albedo measurements, independently of any satellite data. Climatological AOD characteristics could then be used in estimating the site specific atmospheric effect.

5 Conclusions

A robust method was developed for estimating the effect of the atmosphere on broadband surface albedo values measured using ground based pyranometers. The input values needed are the incoming and reflected radiation values and aerosol optical depth values at two wavelengths. Although the method was developed in the needs of validation of satellite based albedo estimates, it is not dependent on any satellite instrument. It provides a possibility to separately study the effect of the atmosphere on the satellite albedo products without complication of the heterogeneity of land cover.

The effect of the atmosphere on the measured broadband surface albedo can be as high as 20 %. The size of the error depends on the sun zenith angle and the atmospheric optical depth.

Acknowledgements. The authors thank Fred Bosveld and Wouter Knap (KNMI, De Bilt, The Netherlands) for the Cabauw surface albedo data. The AOD data made available by AERONET is gratefully acknowledged. The work was financially supported by EUMETSAT in the project Satellite Application Facility on Climate Monitoring.

AMTD
5, 385–409, 2012

References

Ångström, A.: On the Atmospheric Transmission of Sun Radiation and on Dust in the Air, Geogr. Ann., 11, 156–166, 1929.

ASTM Standard G173-03: Standard Tables for Reference Solar Spectral Irradiances: Direct Normal and Hemispherical on a 37 Tilted Surface, ASTM Standard G173-03, American Society for Testing and Materials, West Conshohocken, PA, June 1999.

Bird, R. E. and Riordan, C.: Simple Solar Spectral Model for Direct and Diffuse Irradiance on Horizontal and Tilted Planes at the Earth's Surface for Cloudless Atmospheres, J. Clim. Appl. Meteorol., 25, 87–97, 1986.

Briegleb, B. P., Minnis, P., Ramanathan, V., and Harrison, E.: Comparison of Regional Clear-Sky Albedos Inferred from Satellite Observations and Model Computations, J. Clim. Appl. Meteorol., 25, 214–226, 1986.

Carrer, D., Geiger, B., Roujean, J.-L., Hautecoeur, O., Cedilnik, J., Mahfouf, J.-F., Meurey, C., and Franchisteguy, L.: Land surface albedo from MSG/SEVIRI: Retrieval method, validation, and application for weather forecast, Proc. IGARSS'09 IV, 288–291, 2009.

Clark, R. N. , Swayze, G. A., Wise, R., Livo, K. E., Hoefen, T. M., Kokaly, R. F., and Sutley, S. J.: USGS Digital Spectral Library splib06a, U.S. Geological Survey, Data Series 231, 2007

Govaerts, Y. M., Pinty, B., Taberner, M., and Lattanzio, A.: Spectral Conversion of Surface Albedo Derived From Meteosat First Generation Observations, IEEE Geosci. Remote Sens. Lett., 3, 23–27, 2006.

Gueymard, C.: SMARTS, A Simple Model of the Atmospheric Radiative Transfer of Sunshine: Algorithms and Performance Assessment, Professional Paper FSEC-PF-270-95, Florida Solar Energy Center, 1679 Clearlake Rd., Cocoa, FL 32922, 1995.

Gueymard, C.: Parameterized Transmittance Model for Direct Beam and Circumsolar Spectral Irradiance, Solar Energy, 71, 325–346, 2001.

Holben, B. N., Eck, T. F., Sluster, I., Tanré, D., Buis, J. P., Setzer, A., Vermote, E., Reagan, J. A., Kaufman, Y. J., Nakajima, T., Lavenu, F., Jankowiak, I., and Smirnov, Z.: AERONET – A Federated Instrument Network and Data Archive for Aerosol Characterization, Remote Sens. Environ., 66, 1–16, 1998.

Knap, Wouter: http://www.knmi.nl/bsrn/, last access: 21 December 2011.

Lewis, P. and Barnsley, M. J.: Influence of the sky radiance distribution on various formulations of the Earth surface albedo, in Proc. Conf. Phys. Meas. Sign. Remote Sens., Val d'Isere,

AMTD
5, 385–409, 2012

France, 707–715, 1994.
Liang, S., Shuey, C. J., Russ, A. L., Fang, H., Chen, M., Walthall, C. L., Daughtry, C. S. T., and Hunt Jr., R.: Narrowband to broadband conversions of land surface albedo, II Validation, Remote Sens. Environ., 84, 25–41, 2002.
Lucht, W., Hyman, A. H., Strahler, A. H., Barnsley, M. J., Hobson, P., and Muller, J.-P.: A Comparison of Satellite-Derived Spectral Albedos to Ground-Based Broadband Albedo Measurements Modeled to Satellite Spatial Scale for a Semidesert Landscape, Remote Sens. Environ., 74, 85–98, 2000.
Lyapustin, A., Martonchik, J., Wang, Y., Laszlo, I., and Korkin, S.: Multiangle implementation of atmospheric correction (MAIAC): 1. Radiative transfer basis and look-up tables, J. Geophys. Res., 116, D014985, doi:10.1029/2010JD01, 2011a.
Lyapustin, A., Wang, Y., Laszlo, I., Kahn, R., Korkin, S., Remer, L., Levy, R., and Reid, J. S.: Multiangle implementation of atmospheric correction (MAIAC): 1. Aerosol algorithm, J. Geophys. Res., 116, D03211, doi:10.1029/2010JD014986, 2011b.
Manninen, T. and Riihelä, A.: Atmospheric effect on validation of broadband surface albedo (SAL) product of CM SAF using mast measurements, EUMETSAT Meteorological satellite conference, 8–12 September 2008, CD, Darmstadt, p.8, 2008.
Martonchik, J. V., Diner, D. J., Pinty, B., Verstraete, M. M., Myneni, R. B., Knyazikhin, Y., and Gordon, H. R.: Determination of land and ocean reflective, radiative, and biophysical properties using multiangle imaging, IEEE T. Geosci. Remote, 36, 1266–1281, 1998.
Michalsky, J. J., Harrison, L. C., and Berkheiser III, W. E.: Cosine response characteristics of some radiometric and photometric sensors, Solar Energy, 54, 397–402, 1995.
MODIS BRDF/Albedo Product: Algorithm Theoretical Basis Document, Version 5.0, PIs edited by: Strahler, A. H. and Muller, J.-P., April 1999.
Ohmura, A., Dutton, E., Forgan, B., Frohlich, C., Gilgen, H., Hegne, H., Heimo, A., Konig-Langlo, G., McArthur, B., Muller, G., Philipona, R., Whitlock, C., Dehne, K., and Wild, M.: Baseline Surface Radiation Network (BSRN/WCRP): New precision radiometery for climate change research, B. Am. Meteorol. Soc., 79, 2115–2136, 1998.
Pinty, B., Lattanzio, A., Martonchik, J. V., Verstraete, M. M., Gobron, N., Taberner, M., Widlowski, J.-L., Dickinson, R., and Govaerts, Y.: Coupling Diffuse Sky Radiation and Surface Albedo, J. Atmos. Sci., 62, 2580–2591, 2005.
Pinty, B., Lavergne, T., Voßbeck, M., Kaminski, T., Aussedat, O., Giering, R., Gobron, N., Taberner, M., Verstraete, M. M., and Widlowski, J.-L.: Retrieving surface parameters for

AMTD
5, 385–409, 2012

climate models from Moderate Resolution Imaging Spectroradiometer (MODIS)-Multiangle Imaging Spectroradiometer (MISR) albedo products, J. Geophys. Res., 112, D10116, doi:10.1029/2006JD008105, 2007.

Rahman, H. and Dedieu, G.: SMAC: A simplified method for the atmospheric correction of satellite measurements in the solar spectrum, Int. J. Remote Sens., 15, 123–143, 1994.

Raïch, A., González, J. A., and Calbó, J.: Effects of solar height, cloudiness and temperature on silicon pyranometer measurements, Tethys, 4, 11–18, 2007.

Riihelä, A., Laine, V., Manninen, T., Palo, T., and Vihma, T.: Validation of the Climate-SAF surface broadband albedo product: Comparisons with in situ observations over Greenland and the ice-covered Arctic Ocean, Remote Sens. Environ., 114, 2779–2790, 2010.

Román, M. O., Schaaf, C. B., Lewis, P., Gao, F., Anderson, G. P., Privette, J. L., Strahler, A. H., Woodcock, C. E., and Barnsley, M.: Assessing the coupling between surface albedo derived from MODIS and the fraction of diffuse skylight over spatially-characterized landscapes, Remote Sens. Environ., 114, 738–760, 2010.

Roujean, J.-L., Leroy, M., and Deschamps, P.-Y.: A Bidirectional Reflectance Model of the Earth's Surface for the Correction of Remote Sensing Data, J. Geophys. Res., 97, 20455–20468, 1992.

Schulz, J., Albert, P., Behr, H.-D., Caprion, D., Deneke, H., Dewitte, S., Dürr, B., Fuchs, P., Gratzki, A., Hechler, P., Hollmann, R., Johnston, S., Karlsson, K.-G., Manninen, T., Müller, R., Reuter, M., Riihelä, A., Roebeling, R., Selbach, N., Tetzlaff, A., Thomas, W., Werscheck, M., Wolters, E., and Zelenka, A.: Operational climate monitoring from space: the EUMETSAT Satellite Application Facility on Climate Monitoring (CM-SAF), Atmos. Chem. Phys., 9, 1687–1709, doi:10.5194/acp-9-1687-2009, 2009.

Strahler, A. H., Lucht, W., Schaaf, C. B., Tsang, T., Gao, F., Li, X., Muller, J.-P., Lewis, P., and Barnsley, M. J.: MODIS BRDF/Albedo Product: Algorithm Theoretical Basis Document Version 5.0, p.53, 1999.

WCRP: Summary report from the 9th session of the Baseline Surface Radiation Network (BSRN), Lindenberg, Germany, 29 May–2 June 2006, WCRP informal report No 1/2007, 54, 2007.

Wu, A., Li, Z., and Cihlar, Z.: Effects of land cover type and greenness on advanced very high resolution radiometer bidirectional reflectances: Analysis and removal, J. Geophys. Res., 100, 9179–9192, 1995.

AMTD
5, 385–409, 2012

Table 1. The values of the regression parameters for the empirical relationship between the simulated pyranometer measured broadband surface albedo and the corresponding broadband black-sky albedo.

Regression parameter	Value
c_1	0.036
c_2	0.034
c_3	−0.000064
c_4	−0.00025

AMTD
5, 385–409, 2012

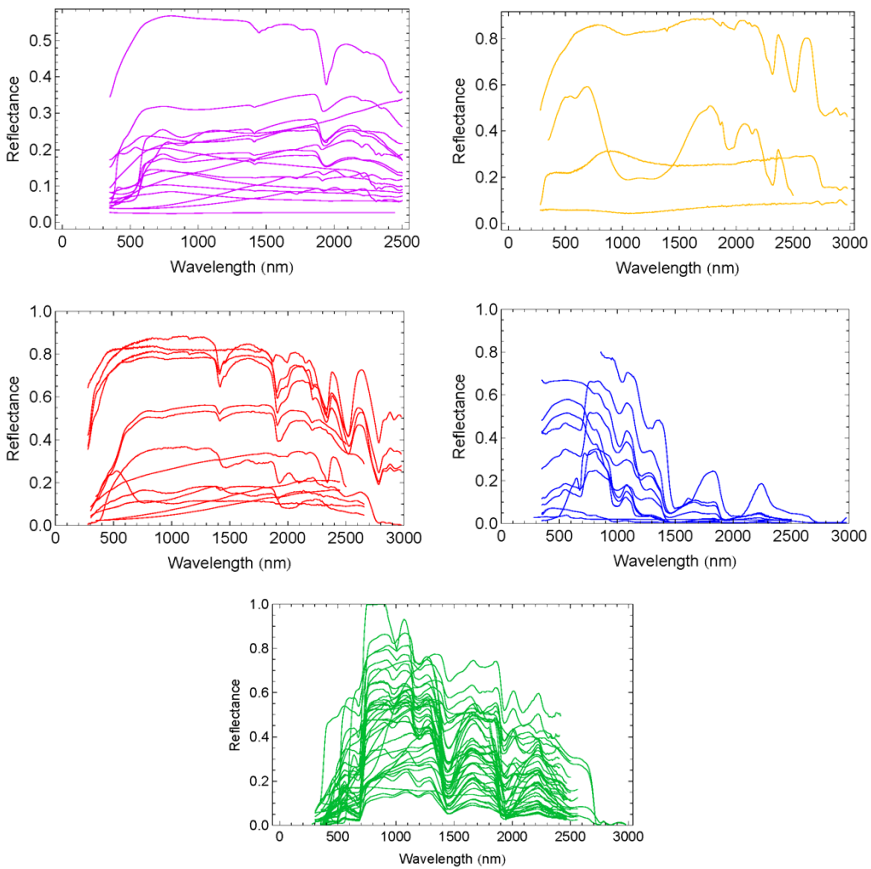

Fig. 1. Reflectance spectra used in the study (Clark et al., 2007). The blue curves represent snow and water, the green curves vegetation, the red curves mixtures, the yellow curves minerals and the lilac curves man-made targets. The snow/water curves contain examples of various melting snow cases, ice and sea water. The vegetation curves contain examples of various tree species, flowers, weeds and grass. The mixtures contain examples of various rocks, such as basalt and limestone. The minerals contain dolomite, magnetite and labradorite sample spectra. The man-made targets are various kinds of asphalt, bricks, rooftar, roofing felt, tarpaper, concrete, woodbeam and dust debris.

AMTD
5, 385–409, 2012

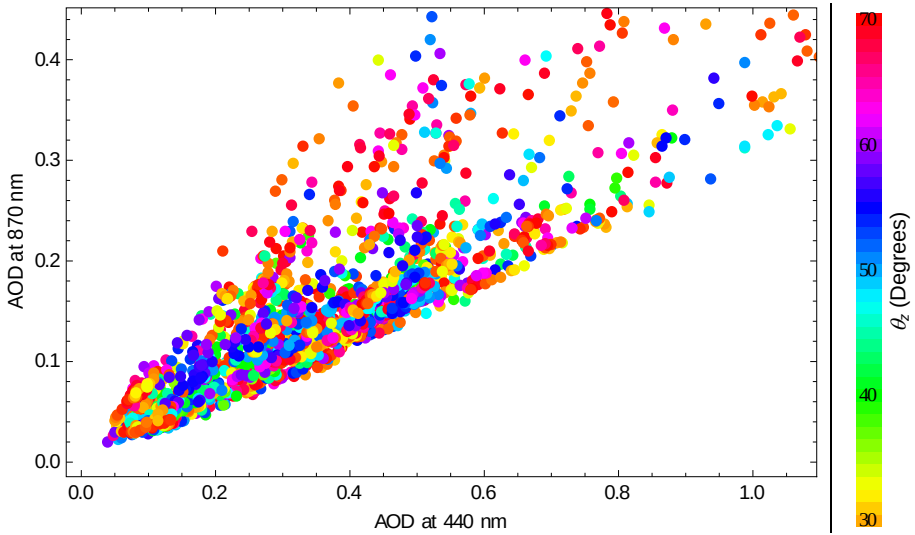

Fig. 2. Aerosol optical depth (AOD) measured at Cabauw during January–September 2007 at wavelengths of 440 nm and 870 nm. The color of the markers varies with the sun zenith angle value as indicated in the color bar.

AMTD
5, 385–409, 2012

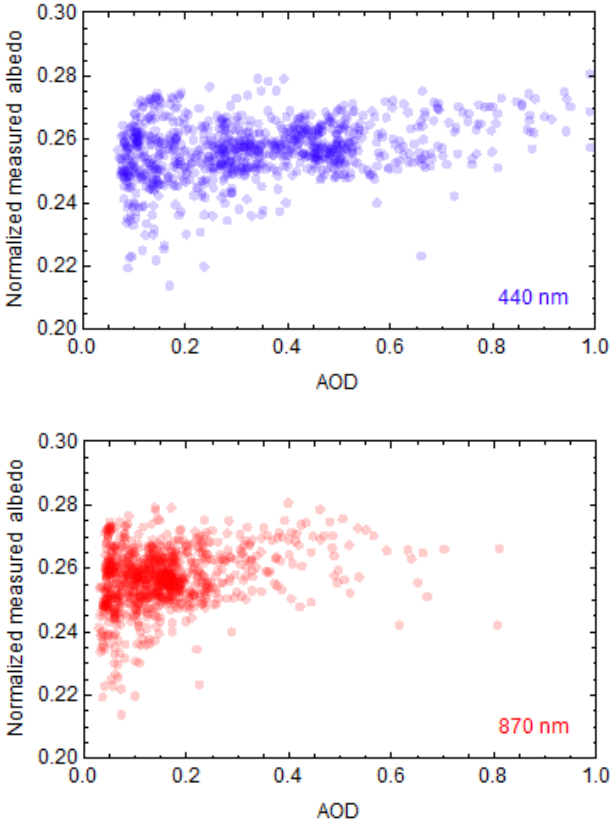

Fig. 3. Measured surface albedo values as a function of aerosol optical depth at wavelengths of 440 nm (blue) and 870 nm (red). The opacity of the symbol is equal for all points. The albedo values are normalized to correspond to the sun zenith angle value of 60°.

AMTD
5, 385–409, 2012

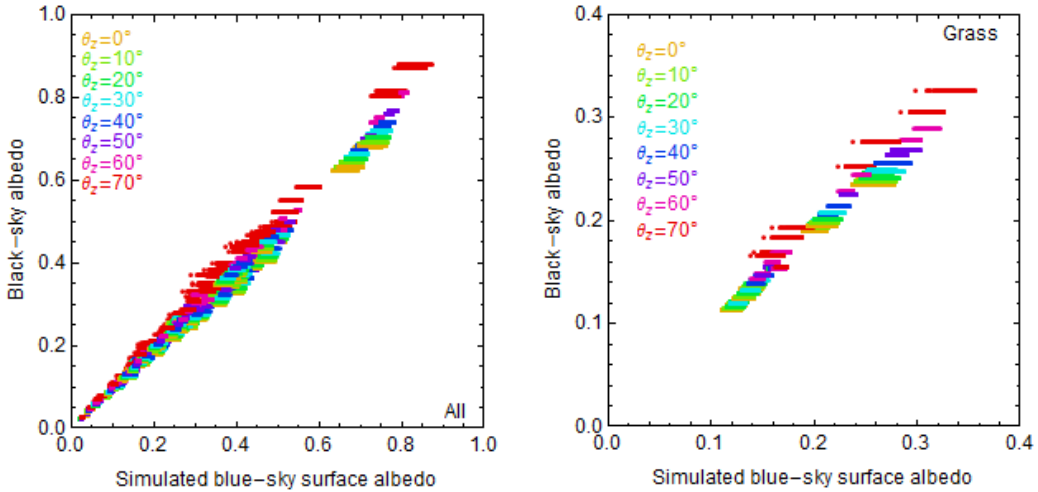

Fig. 4. The calculated black-sky albedo versus corresponding simulated pyranometer measurements of the surface albedo for all 87 land cover spectra (left panel) and all 9 grass spectra (right panel) for all 2226 AOD values measured at Cabauw in January–July 2007. The sun zenith angle values θ_z are colour coded.

AMTD
5, 385–409, 2012

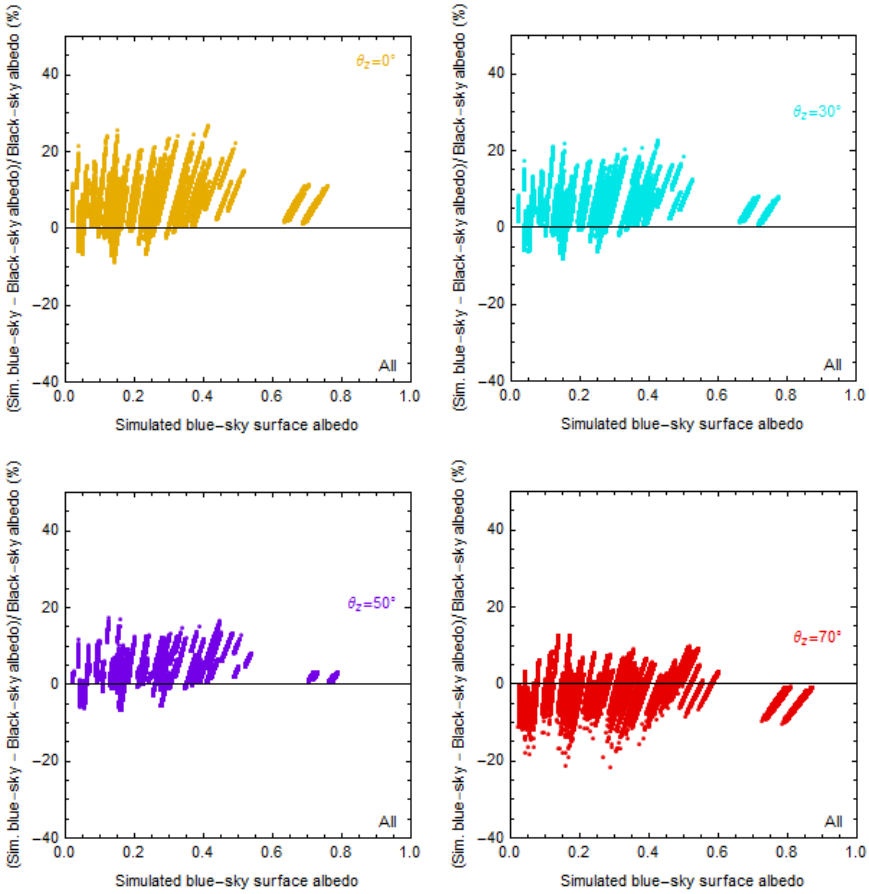

Fig. 5. Calculated black-sky albedo versus corresponding simulated pyranometer measurements of the surface albedo for all 87 land cover spectra used in the studied atmospheres for sun zenith angle values 0° (top left panel), 30° (top right panel), 50° (bottom left panel) and 70° (bottom right panel).

AMTD
5, 385–409, 2012

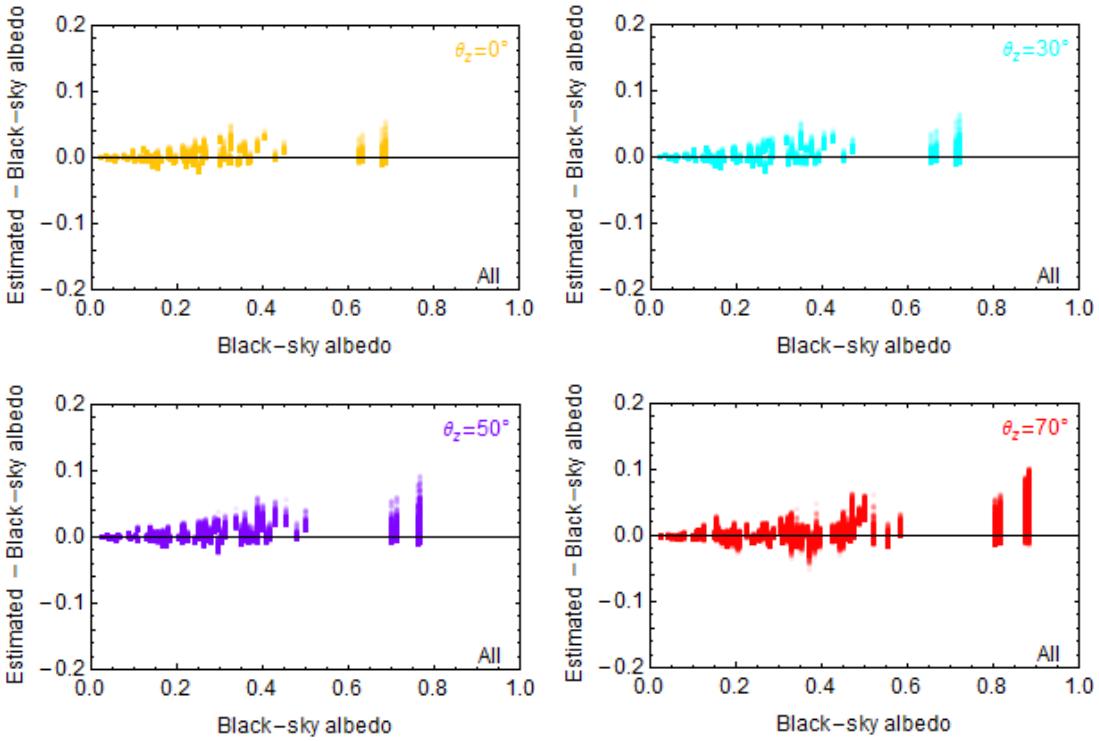

Fig. 6. Difference between the simulated pyranometer measurement estimate of a surface albedo obtained using Eqs. (2) ... (5) and the corrresponding simulated black-sky albedo for the 87 diverse land cover type spectra used in all studied atmospheres and for the sun zenith angle values 0°, 30°, 50° and 70°. The opacity of the points is related to the frequency of the value.

AMTD
5, 385–409, 2012

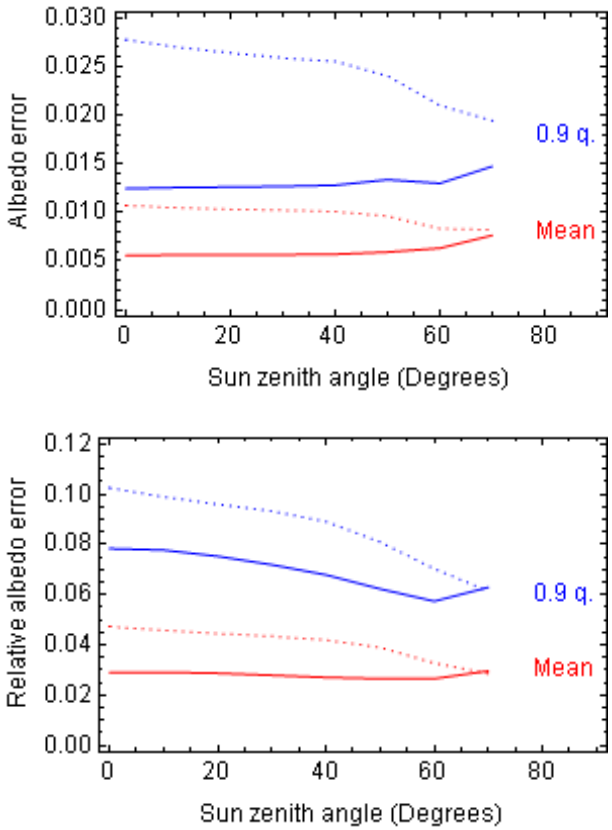

Fig. 7. Deviation (top panel) and relative deviation (bottom panel) of the simulated (Eq. 2) pyranometer measurement of the surface albedo (dashed curves) and its regression based atmospherically corrected (Eq. 6) value (solid curves) from the corresponding calculated black-sky value. The mean and 0.9 quantile values are shown. The curves are based on all 87 spectra and all 2226 AOD values.

AMTD
5, 385–409, 2012

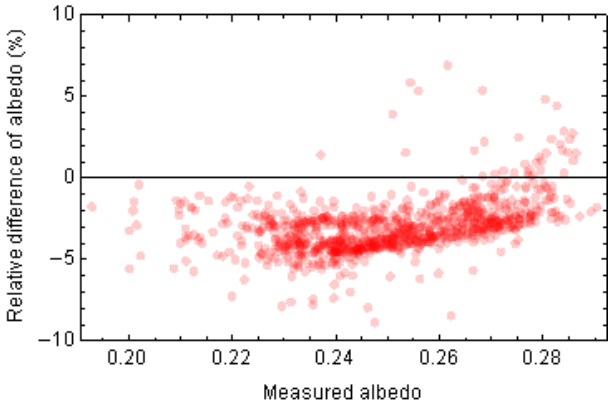

Fig. 8. Relative difference of the atmospherically corrected and uncorrected measured albedo values at Cabauw.

AMTD
5, 385–409, 2012